The Mechanism for Regulation of the F-actin Binding Activity of IQGAP1 by Calcium/Calmodulin*[S]

Scott C. Mateer‡§, Amanda E. McDaniel¶, Valérie Nicolas‖, Geoffrey M. Habermacher,**
Mei-Jung Sun Lin‡‡, Damond A. Cromer‡, Michelle E. King‡§§, and George S. Bloom‡¶¶‖

*From the Departments of ‡Biology and ¶¶Cell Biology, University of Virginia, Charlottesville, Virginia 22903,
¶Cutanix Corporation, Oklahoma City, Oklahoma 73104, ‖Faculté de Pharmacie, Université de Paris-Sud,
Chatenay-Malabry, France, **Emory University School of Medicine, Atlanta, Georgia 30322,
and the ‡‡Department of Cell Biology, University of Texas Southwestern Medical Center, Dallas, Texas 75390*

IQGAP1 colocalizes with actin filaments in the cell cortex and binds *in vitro* to F-actin and several signaling proteins, including calmodulin, Cdc42, Rac1, and β-catenin. It is thought that the F-actin binding activity of IQGAP1 is regulated by its reversible association with these signaling molecules, but the mechanisms have remained obscure. Here we describe the regulatory mechanism for calmodulin. Purified adrenal IQGAP1 was found to consist of two distinct protein pools, one of which bound F-actin and lacked calmodulin, and the other of which did not bind F-actin but was tightly associated with calmodulin. Based on this finding we hypothesized that calmodulin negatively regulates binding of IQGAP1 to F-actin. This hypothesis was tested *in vitro* using recombinant wild type and mutated IQGAP1s and in live cells that transiently expressed IQGAP1-YFP. *In vitro*, the affinity of wild type IQGAP1 for F-actin decreased with increasing concentrations of calmodulin, and this effect was dramatically enhanced by Ca^{2+} and required the IQ domains of IQGAP1. In addition, we found that calmodulin bound wild type IQGAP1 much more efficiently in the presence of Ca^{2+} than EGTA, and all 8 IQ motifs in each IQGAP1 dimer could bind calmodulin simultaneously. In live cells, IQGAP1-YFP localized to the cell cortex, but elevation of intracellular Ca^{2+} reversibly induced the fluorescent fusion protein to become diffusely distributed. Taken together, these results support a model in which a rise in free intracellular Ca^{2+} promotes binding of calmodulin to IQGAP1, which in turn inhibits IQGAP1 from binding to cortical actin filaments.

Actin filament organization in the cell is regulated by a diverse set of factors that collectively control actin polymerization, actin filament length, interfilament cross-links, and interactions of polymerized actin with other cytoskeletal systems and membranes. One such regulatory factor, IQGAP1, is a widely expressed mammalian protein that was first cloned from a human cDNA library using PCR primers to conserved regions within the catalytic domain of Ras GTPase-activating proteins (GAPs)[1] (1). Analysis of its predicted amino acid sequence revealed that the IQGAP1 polypeptide does contain a GAP-related domain, as well as four putative calmodulin-binding IQ motifs (1). Although the GAP-related domain of IQGAP1 does not seem to have GAP catalytic activity (1, 2), it does form part of a region that preferentially binds to activated forms of the small G proteins, Cdc42 and Rac1 (2–4). IQGAP1 consists of two identical 190-kDa subunits that associate with cortical actin filaments in cultured mammalian cells and cross-links actin filaments into bundles and gels *in vitro* (2, 5–7). In addition to its association with actin filaments and the small G proteins, IQGAP1 was found to be the major protein in cultured human breast cell lysates to bind immobilized calmodulin in the absence of calcium (8). Subsequently, a high affinity calmodulin-binding site was mapped to its IQ motifs (9).

The IQGAP1 polypeptide is characterized by the specific arrangement of several modular motifs. An F-actin-binding calponin homology domain is found near its N terminus and is sequentially followed by six imperfect, putative coiled-coil repeats, a WW domain, four IQ motifs, and a GAP-related domain. Several proteins that are structurally related to IQGAP1 have been described. The most similar proteins in terms of primary sequence and domain organization are IQGAP2, a liver-enriched protein in mammals (3, 10), and a *Hydra* protein that has been implicated in tentacle formation (11). Additional IQGAP1-related proteins have been found in *Dictyostelium* (12–14), and *Saccharomyces cerevisiae* (15–17). Although some of these proteins do not contain every major structural motif of IQGAP1, they are sufficiently similar to IQGAP1 to be classified as members of the IQGAP protein family.

In addition to binding F-actin, Cdc42, Rac1, and calmodulin, IQGAP1 has also been reported to bind β-catenin (18), E-cadherin (18, 19), and myosin essential light chain (20). In light of its numerous structural motifs and binding partners, it seems likely that the integration of input from multiple signaling pathways determines which proteins are bound to IQGAP1 at any moment. Supporting this idea is the competitive binding to IQGAP1 that has been described between Ca^{2+}/calmodulin and activated Cdc42 (8, 9), Ca^{2+}/calmodulin and E-cadherin (19), and activated Cdc42 or Rac1 and β-catenin (21).

Similarly, we reported previously (5) that exogenous calmod-

[1] The abbreviations used are: GAPs, GTPase-activating proteins; CHD, calponin homology domain; HBSS, Hanks' balanced salt solution; UTR, untranslated region; TEMED, *N,N′,N′*-tetramethylethylenediamine.

ulin modestly inhibited binding of F-actin to native IQGAP1 purified from bovine adrenal tissue. In the present report, we describe our more recent efforts to clarify how calmodulin influences the binding of IQGAP1 to F-actin. The protein contents of F-actin-binding and non-binding pools of native IQGAP1 were analyzed in further detail. In addition, recombinant full-length and mutant versions of human IQGAP1 were assayed for interactions with calmodulin in the absence and presence of free Ca^{2+} and with F-actin in the absence and presence of free Ca^{2+}, calmodulin, and Ca^{2+}/calmodulin. The net results of this study suggest that local rises in free intracellular Ca^{2+} stimulate binding of calmodulin to the IQ motifs on IQGAP1, which in turn reduces the affinity of IQGAP1 for actin filaments.

EXPERIMENTAL PROCEDURES

Supplies—Biochemical, molecular biological, immunochemical, and tissue culture reagents used for this study and their respective vendors are as follows: A23187 Ca^{2+} ionophore and bovine calmodulin (Calbiochem); Sf9 cells, insect cell media, insect cell antibiotics, the Bac-to-Bac HT expression system, Elongase Amplification System, and the pFast-BAC HT vector (Invitrogen); the bacterial strain, BL21DE3, and the pRSET expression vectors (Invitrogen); Tris, TEMED, 40% acrylamide solution (37.5:1), and 2-mercaptoethanol (Bio-Rad); AlexaFluor 488-phalloidin (Molecular Probes, Eugene, OR); secondary antibodies (Kirkegaard & Perry, Gaithersburg, MD); the pSL1180 vector and calmodulin-Sepharose (Amersham Biosciences); the pBlueScript II SK(+) plasmid (Stratagene, La Jolla, CA); restriction enzymes (New England Biolabs, Beverly, MA); oligonucleotides (Integrated DNA Technologies, Inc., Coralville, IA); the BacPAK Baculovirus Rapid Titer kit and pEY-FPN1 mammalian expression vector (CLONTECH, Palo Alto, CA); Centriprep concentrators (Millipore Corp., Bedford, MA); Slide-A-Lyzer dialysis cassettes and GelCode Blue staining reagent (Pierce); nickel-nitrilotriacetic acid-agarose purification resin (Qiagen, Valencia, CA); anti-calmodulin monoclonal antibody (Upstate Biotechnology, Inc., Lake Placid, NY); Dulbecco's minimum essential medium, and LipofectAMINE Plus (Invitrogen); cosmic calf serum (HyClone, Logan, UT); [α-^{32}P]GTP (ICN, Irvine, CA); Expand Long Template PCR System (Roche Molecular Biochemicals); pGEM-T Easy vector I (Promega, Madison, WI). Unless otherwise stated, all other reagents and chemicals were acquired from Sigma.

Mutagenesis of IQGAP1—A pBlueScript II SK(+) plasmid containing the human cDNA for IQGAP1 (pBSIQG1-MH) was kindly provided by Dr. Matt Hart of Onyx Pharmaceuticals. This plasmid was digested with *Xba*I, and the 694-bp insert containing a portion of the 3′-UTR sequence was removed, and the remaining cDNA was ligated together to form pBSIQG1-2. Next the 5′-UTR was removed by digesting pBSIQG1-2 with *Nco*I and *Xho*I. This produced a 523-bp insert that contained not only the 5′-UTR but also 365 nucleotides of the 5′-coding region. The 523-bp insert was removed, and the remaining vector fragment was ligated to a similarly digested 371-bp PCR fragment (see under "PCR Amplification of DNA") that restored the 365 nucleotides of the coding region and introduced an *Xho*I restriction site 5′ to the start codon. We took the resulting plasmid (pBSIQG-10) and performed a *Xho*I/*Xba*I double digest, purified the ~5500-bp fragment, and ligated it into a similarly digested pSL1180 vector generating the pSLIQG-1 plasmid. Next, to remove the remaining 3′-UTR, the pSLIQG-1 plasmid was digested with *Kpn*I and *Xba*I, and the vector was purified away from an ~1100-bp insert. Because this digest removed not only the 3′-UTR but also 500 nucleotides of C-terminal coding region, the purified vector fragment was ligated onto a similarly digested 500-bp PCR fragment (see under "PCR Amplification of DNA") to restore the missing coding region and to introduce 3 stop codons and an *Xba*I site (pSLIQG-2). Finally, pSLIQG-2 was digested with *Xho*I and *Xba*I; the 6500-bp insert was purified and then ligated into a pFastBAC HT vector that had been digested with *Sal*I and *Xba*I. The resulting plasmid (pFBIQG1) was then used to generate baculovirus expressing IQGAP1$_{FL}$, the full-length wild type protein (see under "Generation of IQGAP1-containing Baculovirus Particles").

To generate the IQGAP1$_{\Delta IQ}$ mutant, which lacks the four contiguous IQ motifs but is otherwise identical to IQGAP1$_{FL}$, we first digested the pSL1180 vector with *Bgl*II and *Bam*HI, removed the 31-nucleotide insert, and ligated the vector together creating the vector pSLΔBglII/*Bam*HI. Next, pSLIQG-2 was digested with *Xho*I and *Xba*I, and the resulting 6500-bp IQGAP1 fragment was purified and ligated into sim-

ilarly digested pSLΔBglII/*Bam*HI plasmid to generate pSLIQG-5. The pSLIQG-5 plasmid was then digested with *Bam*HI and *Sac*I, and a 1241-bp insert fragment was removed. The *Bam*HI/*Sac*I digest removed the region of IQGAP1 that encoded the IQ domain region (amino acids 747–862). To restore amino acids 447–746, PCR was used to amplify the cDNA encoding this region (see under "PCR Amplification of DNA"). The DNA primers used for this amplification introduced a *Bam*HI site by creating a silent mutation in the codon for Glu-746 (GAA was changed to GAG) and contained a *Sac*I site. The resulting PCR product was digested with *Bam*HI and *Sac*I, gel-purified, and then ligated into the purified pSLIQG-5 vector to generate pSLIQG1-ΔIQ. Finally, pSLIQG1-ΔIQ was digested with *Xho*I and *Xba*I, and the ~6100-bp insert fragment was purified and ligated into the pFastBAC HT vector that had been digested with *Sal*I and *Xba*I. The resulting plasmid (pFBIQG1-ΔIQ) was then used to generate baculovirus encoding IQGAP1$_{\Delta IQ}$ (see under "Generation of IQGAP1-containing Baculovirus Particles").

To generate the IQGAP1-(2–522) protein fragment, we utilized a second plasmid given to us by Matt Hart, in which the IQGAP1-coding region had been N-terminally fused in-frame to the Myc epitope tag. In this plasmid the start codon was changed from ATG to GGA to create a *Bam*HI site. Digestion of this plasmid with *Bam*HI and *Hin*dIII generated a 1567-bp fragment that was ligated into the pRSET vector to generate pRSETIQG1-(2–522). This plasmid was then used to express recombinant protein in bacteria (see under "Expression and Purification of Proteins").

PCR Amplification of DNA—By using pBSIQG1-MH as a template and primers 5′-CCGCTCGAGATGTCCGCCGCAGACGAG-3′ (forward primer) and 5′-CTCATCCATGGCATTCAACTGAAT-3′ (reverse primer), PCR was used to generate a DNA fragment that introduced an *Xho*I site 5′ to the start codon and to amplify the 5′ 365-bp coding region. Plasmid pBSIQG1-MH and primers 5′-CGGAGGTACCGACAGAGGA-GAAAGGCC-3′ (forward primer) and 5′-GCTCTAGACTATCATTACT-TCCCGTAGAACTT-3′ (reverse primer) were used to amplify 500 nucleotides from the 3′ end of IQGAP1 and to introduce 3 stop codons and an *Xba*I site 3′ to the coding region. Finally, to restore the region of IQGAP1 encoding amino acids 447–862, plasmid pSLIQG-2 and primers 5′-CACCCAGAGCTCTCTGTCGCAGTGGA-3′ (forward primer) and 5′-CGCGGATCCTCATTGGCCAGCCACAGCTG-3′ (reverse primer) were used to generate a DNA fragment that contained a *Sac*I site at its 5′ end and introduced a *Bam*HI site at its 3′ end by creating a silent mutation in the codon for Glu-746 (GAA was changed to GAG). All PCRs used the reagents and protocols of the Elongase Amplification System. The size of each PCR product was verified by agarose gel electrophoresis and gel-purified.

Generation of IQGAP1-containing Baculovirus Particles—Baculoviruses expressing either IQGAP1$_{FL}$ or IQGAP1$_{\Delta IQ}$ were generated following the procedures and protocols of the Bac-to-Bac HT expression system. Protein expression was verified by Western blotting and immunofluorescence using IQGAP1-specific antibodies. The virus titer was determined by the University of Virginia Tissue Culture Facility using the BacPAK Baculovirus Rapid Titer Kit.

Expression and Purification of Proteins—Actin was purified from rabbit muscle, as described previously (5), and was stored as G-actin in small aliquots at −80 °C. When needed, G-actin was polymerized to generate actin filaments (5) and stored on ice at 4 °C. Native IQGAP1 was purified from bovine adrenal glands by a modification of a method described previously (8). Briefly, 20–30 adrenal glands were harvested and placed in cold TES buffer: 50 mM Tris, pH 7.4, 1 mM EGTA, 300 mM sucrose, 1 mM DL-dithiothreitol, 0.1 mM, phenylmethylsulfonyl fluoride, and a protease inhibitor mixture containing 10 μg/ml each of leupeptin, chymostatin, and pepstatin A. The glands were diced and homogenized, and the resulting slurry was then centrifuged at 10,000 rpm (g_{max} = 16,374 × g) in a Sorval RC-5B centrifuge using the GSA rotor for 30 min. Supernatants were then centrifuged an additional 90 min at 40,000 rpm (g_{max} = 186,000 × g) using the 45Ti rotor and a Beckman L8−80 ultracentrifuge. Next, the resulting supernatant was passed through a 0.45-μm filter, aliquoted, and either snap-frozen for later use or applied to a calmodulin-Sepharose column. Freshly prepared or thawed supernatant was supplemented with NaCl to 150 mM and Triton X-100 to 1% before being applied to the column, which was equilibrated with TENT buffer (TES buffer lacking sucrose, but containing 150 mM NaCl and 1% Triton X-100). The flow-through was discarded; the column was then washed extensively with TEN buffer (TEN, 50 mM Tris, pH 7.4, 150 mM NaCl, 1 mM EGTA, 1 mM DL-dithiothreitol, 0.1 mM, phenylmethylsulfonyl fluoride, and a protease inhibitor mixture containing 10 μg/ml each of leupeptin, chymostatin, and pepstatin A) (TES lacking sucrose, but containing 150 mM NaCl),

and bound protein was eluted with TENS buffer (TEN supplemented with 1 M NaSCN). Eluted fractions were monitored by immunoblotting for IQGAP1, and fractions containing IQGAP1 were pooled and concentrated using 30,000 molecular weight cut-off Amicon Centriprep concentrators following the manufacturer's protocol. The concentrated material was then placed into 10,000 molecular weight cut-off Slide-A-Lyzer dialysis cassettes, dialyzed extensively against TEN buffer, aliquoted, and stored at −80 °C.

Recombinant IQGAP1$_{FL}$ and IQGAP1$_{\Delta IQ}$ were produced using the baculovirus expression system. Briefly, exponentially growing Sf9 cells were infected with appropriate viruses (multiplicity of infection of at least 3). Infected cultures were incubated on a orbital shaker at 27 °C for 48–60 h. The cultures were then centrifuged in a Sorval RC-5B centrifuge using the SLA-1500 rotor at 8,500 rpm (g_{max} = 10,976 × g) for 30 min. The pellets were then either lysed immediately or stored at −80 °C. To lyse cells, pellets were resuspended in lysis buffer (50 mM NaH$_2$PO$_4$ pH 8.0, 10 mM imidazole, 300 mM NaCl, 5 mM 2-mercaptoethanol) and sonicated. Next, cell suspensions were centrifuged in a Sorval RC-5B centrifuge using SA-600 rotor at 10,500 rpm (g_{max} = 15,960 × g) for 30 min. The supernatant was then batch absorbed onto nickel-nitrilotriacetic acid-agarose resin that had been equilibrated previously with lysis buffer. The resin was then washed with several resin volumes of wash buffer A (50 mM NaH$_2$PO$_4$, pH 8.0, 300 mM NaCl, 20 mM imidazole, and 5 mM 2-mercaptoethanol) followed by several washes with wash buffer B (50 mM NaH$_2$PO$_4$, pH 8.0, 300 mM NaCl, 20 mM imidazole, 500 mM NaSCN, 5 mM 2-mercaptoethanol). The bound material was then removed with elution buffer (50 mM NaH$_2$PO$_4$, pH 8.0, 300 mM NaCl, 250 mM imidazole, 5 mM 2-mercaptoethanol). The eluate was placed into 10,000 molecular weight cut-off Slide-A-Lyzer cassettes and dialyzed against several changes of dialysis buffer (50 mM NaH$_2$PO$_4$, pH 8.0, 300 mM NaCl, and 5 mM 2-mercaptoethanol). Finally, the protein was removed from the cassettes, aliquoted, and stored at −80 °C.

Recombinant IQGAP1-(2–522) was expressed in the BL21DE3 strain of *Escherichia coli*. 10 ml of overnight LB agar plates with ampicillin (100 μg/ml) cultures were inoculated with bacteria containing the pRSETIQG1-(2–522) plasmid from well isolated colonies. The next morning 1.0 liter of LB agar plates with ampicillin (100 μg/ml) cultures were inoculated from the overnight suspension and allowed to grow in an orbital shaker (300 rpm at 37 °C) until the $A_{600\,nm}$ was 0.6–0.8. Protein expression was then induced by the addition of isopropyl β-D-thiogalactopyranoside to 0.5 mM, followed by an additional 4-h incubation. The cultures were then centrifuged for 30 min at 8,000 rpm (g_{max} = 10,415 × g) using the GSA rotor and a Sorval RC-5B centrifuge. The pellets were either resuspended in lysis buffer for purification or stored at −80 °C. After the pellet was resuspended in lysis buffer, lysozyme was added to a final concentration of 1 mg/ml. The suspension was then allowed to incubate for an additional hour on ice. After this point, the purification followed the protocol described above for the purification of IQGAP1$_{FL}$ and IQGAP1$_{\Delta IQ}$.

Actin Pelleting Assay, Falling Ball Viscometry, and Electron Microscopy—Unless otherwise stated, recombinant IQGAP1 proteins were combined in a 1.5-ml centrifuge tube with the stated reagents in TN buffer (TEN buffer lacking EGTA), and incubated for 30 min at 27 °C. F-actin was then added to the reaction mix. The sample was then either allowed to incubate at 27 °C for 30 min for actin pelleting assays or drawn into a 100-μl capillary tube followed by incubation for 30 min at 27 °C for falling ball viscometry. After the 30-min incubation, the actin pelleting samples were centrifuged for 20 min at 40,000 rpm (g_{max} = 87,000 × g) using the Beckman Optima TLX ultracentrifuge and the TLA 100.3 rotor. The supernatant fraction was transferred to a fresh centrifuge tube, and the pellet was resuspended to volume with 1× loading buffer for SDS-PAGE. The samples were then analyzed by SDS-PAGE (22), followed either by staining with GelCode Blue or by immunoblotting with anti-IQGAP1 antibodies. Falling ball viscometry and negative stain electron microscopy were performed as described earlier (5).

Antibody Production, Immunoblots, Immunoprecipitation, and GTP Overlays—The polyclonal antibody to IQGAP1 was produced by immunizing a rabbit with IQGAP1-(2–522) and was used either as unfractionated diluted serum or as bulk IgG purified from serum using protein A-Sepharose beads. The IQGAP1 monoclonal IgG2a antibody was produced by footpad immunization of Balb/c mice with purified native bovine adrenal IQGAP1 and fusion of popliteal lymph node cells with NS-1 mouse plasmacytoma cells. The fusion and selection protocol was essentially identical to that used earlier for production of monoclonal antibodies to kinesin (23).

With one modification, protocols described previously were also used

for quantitation of GTP overlay blots (24), gel electrophoresis (5), and immunoblotting (5). The modification was to use a Umax (Freemont, CA) Astra 2200 scanner with a transparency adapter and 12-bit grayscale depth, instead of a CCD camera, to capture digital images of gels and chemiluminescent Western blots. Concentration series of the following purified proteins were used as standards for quantitation: native bovine adrenal IQGAP1, recombinant IQGAP1$_{FL}$, recombinant IQGAP1$_{\Delta IQ}$, native bovine calmodulin, recombinant His$_6$-Cdc42, and recombinant His$_6$-Rac1.

IQGAP1 was immunoprecipitated using the polyclonal IQGAP1 antiserum or IgG purified from the antiserum by protein A-Sepharose affinity chromatography. The antiserum or IgG was added to samples containing IQGAP1, and the resulting mixtures were incubated for 1 h at 27 °C. Next, protein A-Sepharose was added and incubated for an additional hour at 27 °C. After their incubation, the samples were centrifuged for 5–10 s, and the supernatants were removed. The remaining resin was then washed several times with TN buffer. Finally, the beads were suspended in 1× SDS-PAGE sample buffer, heated, and then analyzed by SDS-PAGE and Western blotting.

Light Microscopic Analysis of IQGAP1-YFP and F-actin in Cultured Cells—By using a pBSIQGAP1-2 template and the oligonucleotides, 5′-GTCGACTATGTCCGCCGCAGAC-3′ and 5′-CCCGGGGGGTAGAAC-TTTTTGTT-3′, the entire IQGAP1 sequence was amplified by PCR using the Expand Long Template PCR System. The size of the PCR product was verified by agarose gel electrophoresis. The PCR fragment was then ligated into the pGEM-T Easy vector to produce pGEM-IQGAP1. Finally the pGEM-IQGAP1 plasmid was sequentially digested with *Sal*I and *Sma*I, and the IQGAP1 insert was ligated into a similarly digested pEYFP-N1 expression vector to produce pYFP-IQGAP1.

NIH-3T3 fibroblasts were transiently transfected for IQGAP1-YFP expression using LipofectAMINE Plus according to the vendor's instructions. The cells were maintained in Dulbecco's minimum essential medium supplemented with 10% cosmic calf serum and 50 μg/ml gentamicin sulfate. Live transfected cells were observed and recorded by confocal epifluorescence microscopy on an imaging system containing the following components: a Zeiss Axiovert 100 microscope equipped with a CARV spinning disc confocal head, a temperature-regulated stage, automated shutter, an Atto Arc 100-watt mercury illuminator, and a Hamamatsu (Bridgewater, NJ) Orca-ER cooled CCD. Images captured by the camera were imported into a Power Macintosh G4 computer (Apple; Cupertino, CA) and processed and analyzed using Open Lab 3.0.3 software (Improvision; Lexington, MA). Cells were maintained on the microscope stage in Attofluor Cell Chambers (Atto Instruments; Rockville, MD) at 37 °C in an atmosphere of 95% air plus 5% CO$_2$. Time lapse imaging was controlled by a program designed using the Automator feature of Open Lab. For Fig. 8 and the corresponding on-line QuickTime movies (see the Supplemental Material), Ca^{2+} addition was achieved by replacing the tissue culture medium with Ca^{2+}-free Hanks' balanced salt solution (HBSS) supplemented the Ca^{2+} ionophore, A23187, at 5 μM, plus 1 mM CaCl$_2$. For Ca^{2+} removal, the solution bathing the cells was replaced with Dulbecco's modified Eagle's medium plus 10% Cosmic calf serum. A total of 64 images were captured, 44 during exposure of cells to A23187 plus CaCl$_2$ and 20 during the reversal step. For both the forward and reverse series, all images were collected at 30-s intervals and were exposed for 10 s each using a 63× planapochromatic Zeiss objective without binning. As controls, comparable experiments were performed using HBSS supplemented with 1 mM CaCl$_2$ or 5 μM A23187 individually. To visualize F-actin, untreated cells, and cells exposed for 20 min to A23187 in the absence or presence of CaCl$_2$ were fixed and labeled with AlexaFluor 488-phalloidin as described earlier for bodipy-phallicidin (5).

RESULTS

Native IQGAP1 Consists of Two Operationally Distinct Protein Pools—Our original method for purifying native IQGAP1 from bovine adrenal tissue was based on ion exchange and gel filtration chromatography and demonstrated copurification of one calmodulin molecule per ~13 IQGAP1 dimers (5). Addition of a large molar excess of exogenous calmodulin to IQGAP1 purified in this manner caused a modest decrease in the ability of IQGAP1 to bind actin filaments (5). These observations prompted us to investigate the mechanism by which calmodulin inhibits the actin binding activity of IQGAP1.

To begin, we modified a procedure based on calmodulin affinity chromatography (8) to develop a new, more efficient method for purifying bovine adrenal IQGAP1 (see "Experimen-
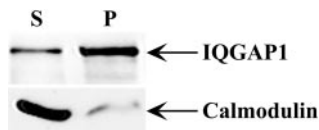
FIG. 1. **Native IQGAP1 consists of two distinct protein pools.** Native IQGAP1 was purified from bovine adrenal tissue, mixed with actin filaments, and then centrifuged. The pellet was resuspended to the original sample volume, and equal aliquots of the supernatant (*S*) and pellet (*P*) fractions were then analyzed by SDS-PAGE. IQGAP1 was detected by staining the gel with GelCode Blue, and calmodulin was detected by anti-calmodulin immunoblotting, and the partitioning of both proteins between the supernatant and pellet fractions was determined by quantitative densitometry. Although ~75% of the IQGAP1 was in the pellet, nearly all of the calmodulin was in the supernatant complexed with IQGAP1 at a 1:1 molar ratio.

tal Procedures"). When native IQGAP1 purified by this new method was mixed with polymerized actin and then centrifuged, quantitative analysis of SDS-polyacrylamide gels and anti-calmodulin Western blots demonstrated that the pellets contained ~75% of the total IQGAP1 but only trace amounts of calmodulin. In contrast, the supernatants contained approximately equimolar amounts of IQGAP1 dimers and calmodulin (Fig. 1). These results raised the possibility that association of calmodulin with IQGAP1 can inhibit the latter's affinity for actin filaments.

The partitioning of calmodulin with the non-actin-binding pool of IQGAP1 could not have been influenced by interactions between IQGAP1 and the small G proteins known to bind to it. This was determined by quantitative Western blotting for Cdc42 and Rac1 of pellets and supernatants from F-actin binding experiments (data not shown). Cdc42 was found in the pellets at a molar ratio to IQGAP1 of less than 1:100 and was undetectable in the supernatants. Rac1, in contrast, could not be detected in either fraction. The sensitivity of these Western blots for Cdc42 and Rac1 was determined as described under "Experimental Procedures" and would have enabled detection of either protein at molar ratios to IQGAP1 of ~1:170 in the supernatants and ~1:500 in the pellets of the F-actin binding experiments.

Production of Recombinant Wild Type and Mutant Versions of IQGAP1—It is evident from our limited analysis of calmodulin and small G proteins that the content of reversibly associating cofactors varies from molecule to molecule of tissue-derived IQGAP1. When one takes into account its other known cofactors, β-catenin and E-cadherin, and the possibility that IQGAP1 can be post-translationally modified in a variety of ways and at multiple sites, IQGAP1 purified from tissue may represent a heterogeneous collection of individual protein complexes. This suspected molecular diversity compromised our efforts to interpret how calmodulin affects the F-actin binding activity of native IQGAP1.

To minimize the molecular heterogeneity of IQGAP1 preparations and enable studies using mutated versions of the protein, we produced three recombinant, His_6-tagged varieties of human IQGAP1 (Fig. 2). $IQGAP1_{FL}$, a full-length protein, and $IQGAP1_{\Delta IQ}$, which lacks the four IQ motifs, were expressed in Sf9 insect cells using modified baculoviruses. IQGAP1-(2–522), which corresponds to amino acids 2–522 of full-length IQGAP1, does not extend beyond the middle of the fourth internal repeat, and therefore does not contain the WW, IQ, or GAP-related domains, was expressed in *E. coli* using a pRSET vector. Following their purification by nickel affinity chromatography, all three proteins were analyzed by quantitative densitometry of GelCode Blue-stained SDS-PAGE gels for recombinant IQGAP1s, of Western blots for calmodulin, and of radiolabeled GTP blots for small G proteins. By using these approaches, the molar ratios of calmodulin to $IQGAP1_{FL}$ and
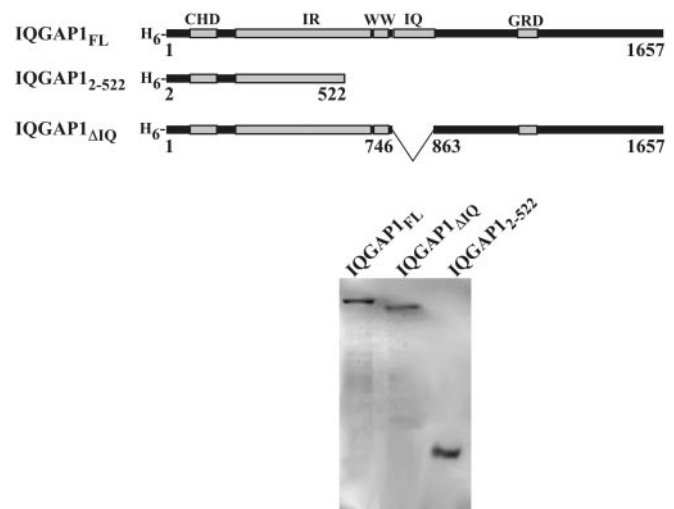

FIG. 2. **Recombinant IQGAP1 proteins.** The three recombinant IQGAP1 proteins used for this study are shown here as diagrammatic representations and in purified forms analyzed by SDS-PAGE. All were expressed as fusion proteins coupled at their N termini to six consecutive histidines (H_6) and were derived from the sequence of human IQGAP1 (1). $IQGAP1_{FL}$, which corresponds to the full-length protein, and $IQGAP1_{\Delta IQ}$, which lacks the four IQ motifs, were expressed in Sf9 insect cells infected with modified baculoviruses. The N-terminal fragment, IQGAP1-(2–522), was expressed in *E. coli* using a pRSET-derived vector. Several protein interaction domains (*shaded regions*) are shown and include the calponin homology domain (*CHD*), the six putative coiled-coil internal repeats (*IR*), the WW domain (*WW*), the four calmodulin binding IQ motifs (*IQ*), and the GAP-related domain (*GRD*). *Numbers below* each diagram denote the N- and C-terminal amino acids for each protein and, additionally in the case of $IQGAP1_{\Delta IQ}$, the first and last amino acids flanking the deleted IQ motifs.

$IQGAP1_{\Delta IQ}$ were found to be ~1:270 and ~1:700, respectively; the molar ratios of small G proteins to $IQGAP1_{FL}$ and $IQGAP1_{\Delta IQ}$ were determined to be ~1:40 and ~1:80, respectively, and neither calmodulin nor small G proteins were detected in purified preparations of IQGAP1-(2–522) (data not shown). In practical terms, the recombinant IQGAP1s were therefore nearly devoid of bound calmodulin, Cdc42, and Rac1.

Calmodulin-sensitive F-actin Binding by IQGAP1 Requires the High Affinity Calmodulin Binding Domains—Previous reports (9) have shown that IQGAP1 contains two putative calmodulin-binding regions, a high affinity site corresponding to its IQ domains and a low affinity site within in its N-terminal 232 amino acids. To determine which calmodulin domain regulates binding of IQGAP1 to actin filaments, the recombinant IQGAP1 proteins were assayed for interactions with F-actin. Fig. 3*A* depicts gelation dose-response curves for $IQGAP1_{FL}$ and IQGAP1-(2–522). Like native IQGAP1 (5), both recombinant proteins were able to gel F-actin, with their critical gelation concentrations being ~200 and ~750 nM for $IQGAP1_{FL}$ and IQGAP1-(2–522), respectively, in the presence of 5 μM polymerized actin.

Next, falling ball viscometry was used to assay the F-actin cross-linking activities of 200 nM $IQGAP1_{FL}$ and 750 nM IQGAP1-(2–522) in the presence of calmodulin, Ca^{2+}, and Ca^{2+}/calmodulin (Fig. 3*B*). The calmodulin concentrations for these experiments were equimolar to the recombinant IQGAP1 proteins, and Ca^{2+} was used at 1 mM. IQGAP1-(2–522) was able to gel 5 μM polymerized actin under all the conditions tested. In the presence of 1 mM EGTA (no Ca^{2+}), $IQGAP1_{FL}$ also formed a gel that was insensitive to calmodulin. In the presence of Ca^{2+}, however, $IQGAP1_{FL}$ was unable to gel F-actin when calmodulin was also present, and the apparent viscosity of such samples was very low, virtually identical to that of F-actin alone. Interestingly, $IQGAP1_{FL}$ did not gel F-

A

B

C
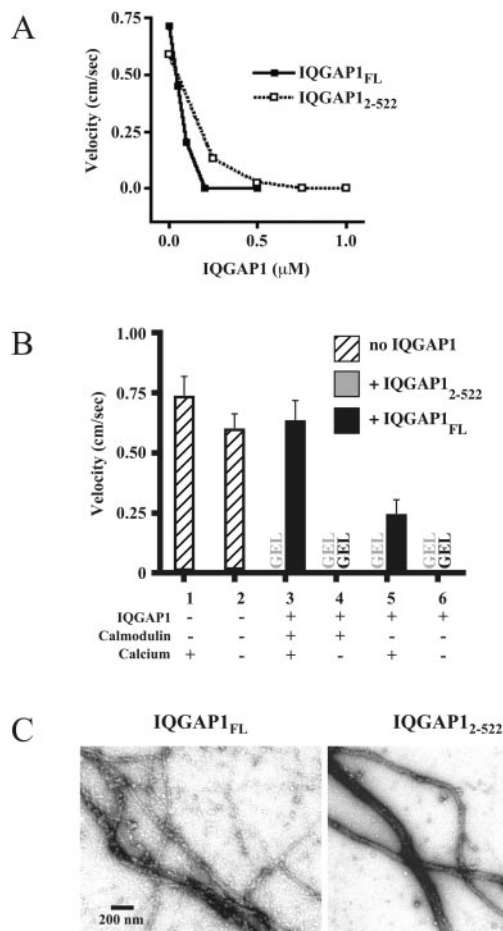
FIG. 3. **The gelation activity of IQGAP1 is sensitive to Ca^{2+}/calmodulin.** *A*, falling ball viscometry was used to measure gelation dose-response curves for $IQGAP1_{FL}$ and IQGAP1-(2–522) in the presence of 5 μM polymerized actin. A velocity of zero indicates the formation of an actin filament gel. The critical concentrations for gelation were determined to be 200 and 750 nM for $IQGAP1_{FL}$ and IQGAP1-(2–522), respectively. *B*, $IQGAP1_{FL}$ (200 nM) or IQGAP1-(2–522) (750 nM) was incubated with 5 μM polymerized actin alone or in the presence of Ca^{2+} (1 mM), calmodulin (equimolar to $IQGAP1_{FL}$ or IQGAP1-(2–522)), or Ca^{2+}/calmodulin as indicated. Samples that lacked Ca^{2+} (*lanes 2, 4,* and *6*) contained 1 mM EGTA. Falling ball viscometry was then used to monitor each sample. In each case, sample viscosity is an inverse function of the measured velocity of the falling ball (*y axis*). Each point represents the mean of at least three separate experiments ± S.D. Note that IQGAP1-(2–522) formed gels under all conditions tested, but gelation by $IQGAP1_{FL}$ was inhibited completely by Ca^{2+}/calmodulin, but only slightly by Ca^{2+} alone and not at all by calmodulin. *C*, both $IQGAP1_{FL}$ and IQGAP1-(2–522) are able to bundle actin filaments, as shown in these negative-stain electron micrographs of samples prepared in the absence of Ca^{2+} or calmodulin.

actin in the presence of Ca^{2+} alone, but the apparent viscosity of such samples was high, and close to the gelation point. The ability $IQGAP1_{FL}$ and IQGAP1-(2–522) to bundle F-actin was also tested. As shown by negative stain electron microscopy in Fig. 3*C*, both recombinant proteins supported F-actin bundle formation in the absence of calmodulin or Ca^{2+}.

As a complement to falling ball viscometry, a high speed pelleting assay was used to monitor the ability of $IQGAP1_{FL}$ and $IQGAP1_{\Delta IQ}$ to bind F-actin. We incubated 0.5 μM $IQGAP1_{FL}$ or $IQGAP1_{\Delta IQ}$ with 1 μM F-actin in the absence or presence of calmodulin, Ca^{2+}, or Ca^{2+}/calmodulin, centrifuged the samples, and then analyzed the supernatant and pellet fractions by quantitative SDS-PAGE. When they were present, calmodulin was equimolar (0.5 μM) or in 10-fold molar excess (5 μM) to $IQGAP1_{FL}$ dimers, and the Ca^{2+} concentration was fixed at 220 μM.

A

B
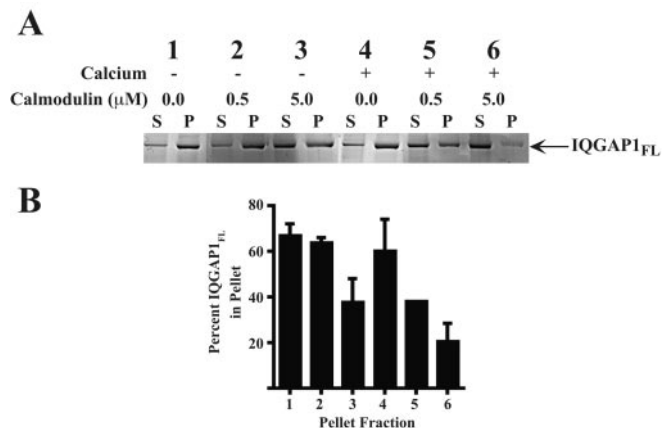
FIG. 4. **Actin filament binding by $IQGAP1_{FL}$, but not $IQGAP1_{\Delta IQ}$, is sensitive to Ca^{2+}/calmodulin.** *A*, 0.5 μM $IQGAP1_{FL}$ was incubated with the indicated amounts of calmodulin in the presence of 220 μM Ca^{2+} or EGTA (no Ca^{2+}) and then was combined with 1 μM polymerized actin. The reaction mixtures were then centrifuged. The pellets were then resuspended to the initial sample volumes, and equal aliquots of the supernatant (*S*) fractions and pellet (*P*) fractions were then subjected to SDS-PAGE. The gel was stained with GelCode Blue. *B*, quantitative densitometry was used to measure the proportion of $IQGAP1_{FL}$ that pelleted out of comparable starting samples. The *numbers* below the *x axis* refer to the corresponding samples in *A*, and the *error bars* indicate the S.D. for data collected from four experiments. The S.D. for sample 5 is not visible on this graph because it was negligible.

Fig. 4, *A* and *B*, summarizes the results for $IQGAP1_{FL}$. In controls, as well as in samples supplemented with Ca^{2+} or equimolar calmodulin alone, ~65% of the $IQGAP1_{FL}$ pelleted with the actin filaments. The amount of pelleted $IQGAP1_{FL}$ dropped to ~40% when either a 10-fold molar excess of calmodulin or Ca^{2+} plus equimolar calmodulin was present. Finally, in the presence of Ca^{2+} plus a 10-fold molar excess of calmodulin, just ~20% of the $IQGAP1_{FL}$ was pelleted. Thus, calmodulin inhibited binding of $IQGAP1_{FL}$ to F-actin, and Ca^{2+} potentiated this activity of calmodulin.

Analogous experiments using $IQGAP1_{\Delta IQ}$ demonstrated that deletion of the high affinity calmodulin binding region from IQGAP1 abolished the ability of Ca^{2+}/calmodulin to inhibit its F-actin binding activity (Fig. 5*A*). In the absence of F-actin, ~10% of $IQGAP1_{\Delta IQ}$ was pelleted by the centrifugation conditions used for these experiments, but addition of actin filaments caused a nearly 4-fold increase in the amount of $IQGAP1_{\Delta IQ}$ found in the pellet fraction. Although $IQGAP1_{\Delta IQ}$ never bound F-actin as efficiently as $IQGAP1_{FL}$ or native bovine adrenal IQGAP1, its affinity for actin filaments was not sensitive to 220 μM Ca^{2+}, 5 μM calmodulin, or a combination of Ca^{2+} plus calmodulin.

The low efficiency binding was evidently due to an inherently reduced affinity for F-actin of $IQGAP1_{\Delta IQ}$, as compared with native IQGAP1, $IQGAP1_{FL}$, or IQGAP1-(2–522). This was determined by demonstrating that the amount of $IQGAP1_{\Delta IQ}$ that could be pelleted in the presence of F-actin steadily increased as the F-actin concentration increased (Fig. 5*B*). Consistent with the evidence that the F-actin binding activity of $IQGAP1_{\Delta IQ}$ was insensitive to calmodulin was the finding that $IQGAP1_{\Delta IQ}$ could not coimmunoprecipitate with calmodulin in either the absence or presence of Ca^{2+} (Fig. 5*C*). Taken together, these results led us to conclude that the IQ motifs of IQGAP1, which correspond to the high affinity calmodulin binding region of the protein (9), account for the F-actin binding sensitivity of IQGAP1 to Ca^{2+}/calmodulin.
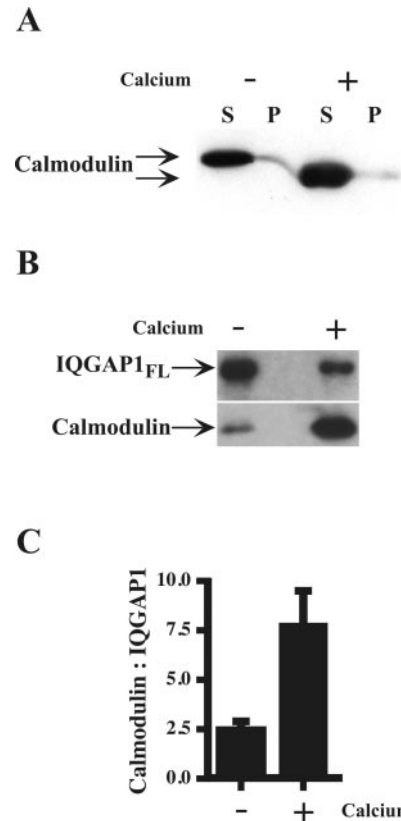
Complexes of IQGAP1 and Ca^{2+}/Calmodulin Bind Poorly to F-actin—The data presented to this point favor the hypothesis
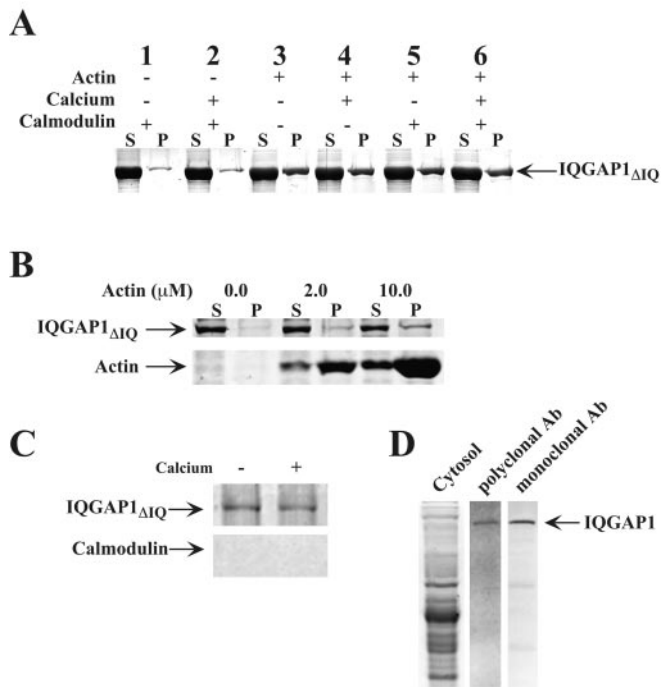
FIG. 5. **Actin filament binding by IQGAP1$_{\Delta IQ}$ is not sensitive to Ca²⁺/calmodulin.** *A*, 0.5 μM IQGAP1$_{\Delta IQ}$ was incubated with or without a 10-fold molar excess of calmodulin in the presence of 220 μM Ca²⁺ or EGTA (no Ca²⁺). The samples were then combined with either buffer (*lanes 1* and *2*) or 1 μM polymerized actin (*lanes 3–6*) and centrifuged. Finally, the pellets were resuspended to the initial sample volumes, and equal aliquots of the supernatant (*S*) and pellet (*P*) fractions were resolved by SDS-PAGE, and the gel was stained with GelCode Blue. Note that in contrast to the case for IQGAP1$_{FL}$ (Fig. 4), the binding of IQGAP1$_{\Delta IQ}$ was completely insensitive to calmodulin or Ca²⁺/calmodulin. *B*, 0.5 μM IQGAP1$_{\Delta IQ}$ was incubated with 0, 2, or 10 μM polymerized actin and then centrifuged and analyzed as in *A*. The amount of IQGAP1$_{\Delta IQ}$ that pelleted increased with increasing actin concentration. This indicates that the relatively poor efficiency with which IQGAP1$_{\Delta IQ}$ binds F-actin was not caused by a high proportion of inactive recombinant protein, but rather because of its reduced affinity for F-actin compared with that of IQGAP1$_{FL}$. *C*, 0.5 μM IQGAP1$_{\Delta IQ}$ was mixed with 5 μM calmodulin in the absence or presence of 220 μM Ca²⁺ and then was immunoprecipitated using polyclonal anti-IQGAP1 IgG. Note that neither immunoprecipitate contained a level of calmodulin that could be detected by anti-calmodulin immunoblotting, although they did contain equivalent levels of IQGAP1$_{\Delta IQ}$, as determined by GelCode Blue staining of an SDS-polyacrylamide gel. Evidently, therefore, IQGAP1$_{\Delta IQ}$ does not bind calmodulin. *D*, polyclonal and monoclonal antibodies made against IQGAP1 were analyzed by immunoblotting of 50-μg aliquots of bovine adrenal cytosol. Note that each antibody reacted most prominently with a band with the electrophoretic mobility of IQGAP1.

FIG. 6. **Ca²⁺ stimulates binding of calmodulin to IQGAP1.** *A*, 0.5 μM IQGAP1$_{FL}$ was incubated with equimolar calmodulin in the presence of 220 μM Ca²⁺ or EGTA (no Ca²⁺) and then combined with 1 μM polymerized actin. The samples were then centrifuged, and the resulting supernatant (*S*) and pellet fractions (*P*) were analyzed by anti-calmodulin immunoblotting. As can be seen, the vast majority of the calmodulin partitioned in the supernatant and calmodulin exhibited a Ca²⁺-dependent gel mobility shift. *B*, supernatants from samples similar to those shown in *A* were immunoprecipitated with a polyclonal antibody against IQGAP1, and the resulting immunoprecipitates were immunoblotted with monoclonal antibodies to either IQGAP1 or calmodulin. Note that IQGAP1$_{FL}$ was tightly associated with a much higher level of calmodulin when Ca²⁺ was present, as opposed to absent. *C*, supernatants from samples similar to those shown in *A* were immunoprecipitated with a monoclonal antibody against the His$_6$ tag present on IQGAP1$_{FL}$. The resulting immunoprecipitates were then analyzed for IQGAP1$_{FL}$ by quantitative SDS-PAGE and for calmodulin by quantitative immunoblotting with anti-calmodulin. The measured molar ratios of calmodulin to IQGAP1$_{FL}$ in the presence or absence of Ca²⁺ are indicated, and each point represents the mean ± S.D. of three experiments. Note that ~3 times as much calmodulin was associated with IQGAP1$_{FL}$ in the presence of Ca²⁺ than in its absence. Furthermore, when Ca²⁺ was present, most IQGAP1$_{FL}$ dimers apparently bound a calmodulin molecule to each of their 8 IQ motifs.

that binding of Ca²⁺/calmodulin to one or more of the eight IQ motifs present in an IQGAP1 dimer can substantially decrease the affinity of that dimer for F-actin. It follows naturally that when IQGAP1 and calmodulin are mixed with F-actin and Ca²⁺, and the solution is then centrifuged, most of the calmodulin should partition in the supernatant. As shown in Fig. 6*A*, this is, indeed, the case. Centrifugation of a mixture of 0.5 μM calmodulin, 0.5 μM IQGAP1$_{FL}$, and 1 μM polymerized actin, in the presence of 220 μM Ca²⁺ or EGTA, yielded supernatants that contained more than 90% of the total calmodulin present in each pair of supernatant and pellet as determined by quantitative Western blotting.

Another prediction of the Ca²⁺/calmodulin hypothesis is that the amount of calmodulin complexed with IQGAP1 should be much greater in Ca²⁺-containing supernatants than in comparable supernatants prepared from samples that lack free Ca²⁺. To test that prediction, supernatant fractions from F-actin-containing samples similar to those shown in Fig. 6*A* were

immunoprecipitated with a polyclonal antibody to IQGAP1, and the immunoprecipitates were then analyzed by immunoblotting with monoclonal antibodies to calmodulin and IQGAP1. As can be seen in Fig. 6*B*, the relative levels of calmodulin to IQGAP1 were much greater in the presence of Ca²⁺ than EGTA. Quantitative analysis of such Western blots indicated that addition of Ca²⁺ caused the amount of calmodulin able to coprecipitate with IQGAP1 to increase 3-fold (Fig. 6*C*), rising from ~2.5 mol of calmodulin per IQGAP1 dimer in the presence of EGTA to ~7.5 mol in the presence of Ca²⁺. This result compares well with a prior report that Ca²⁺ caused a 2-fold increase in the binding of IQGAP1 to calmodulin-Sepharose beads (8). Taken together, these results demonstrate that Ca²⁺ stimulates the binding of calmodulin to IQGAP1 and lend further support to the concept that binding of calmodulin to IQGAP1 inhibits the latter's affinity for actin filaments.

A

B
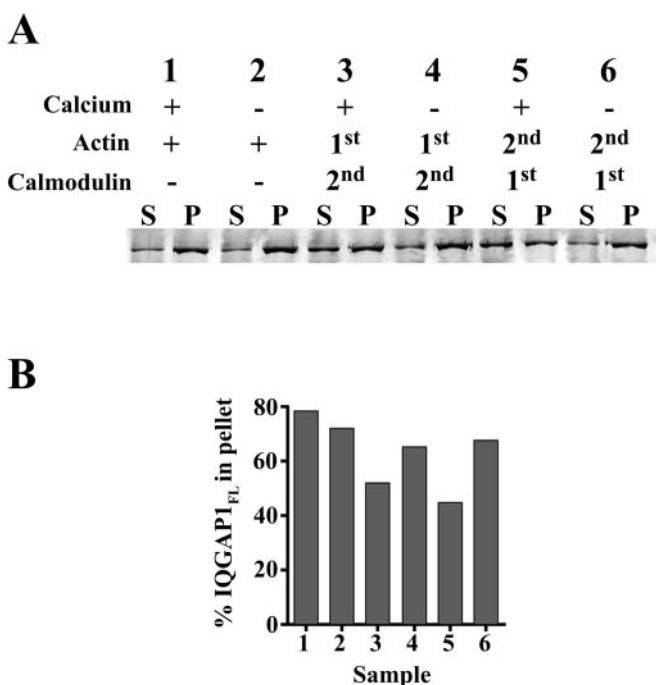
FIG. 7. **Ca^{2+}/calmodulin triggers the release of IQGAP1 from actin filaments.** *A*, 0.5 μM IQGAP1$_{FL}$ was incubated for 30 min with either 1 μM polymerized actin (*lanes 1–4*) or 0.5 μM calmodulin (*lanes 5 and 6*) in the presence of 220 μM Ca^{2+} or EGTA (no Ca^{2+}). Next, the samples were combined with buffer (*lanes 1* and *2*), 0.5 μM calmodulin (*lanes 3* and *4*), or 1 μM polymerized actin (*lanes 5* and *6*). Finally, the reaction mixtures were centrifuged, and the pellets were resuspended to the initial sample volumes. Equal aliquots of the supernatant (*S*) fractions and pellet (*P*) fractions were then subjected to SDS-PAGE, and the gel was stained with GelCode Blue. *B*, quantitative densitometry of the gel shown in *A* was used to measure the proportion of IQGAP1$_{FL}$ that pelleted out of each starting sample. The *numbers below* the *x axis* refer to the corresponding samples in *A*. Note that preincubation of IQGAP1$_{FL}$ with actin filaments did not prevent Ca^{2+}/calmodulin from inhibiting its actin filament binding activity.

Ca^{2+}/Calmodulin Can Displace IQGAP1 from Actin Filaments—All data shown until now were obtained from experiments in which recombinant IQGAP1 proteins were allowed to incubate with Ca^{2+}, calmodulin, or Ca^{2+}/calmodulin for 30 min before F-actin was added. Thus, the IQGAP1 proteins always formed complexes with potential inhibitors of F-actin binding before being exposed to the actin filaments. Our next goal was to determine whether prior association of these recombinant proteins with F-actin prevented formation of such complexes.

Fig. 7 illustrates that the order in which reaction components are mixed together does not alter the ability of Ca^{2+}/calmodulin to inhibit binding of IQGAP1$_{FL}$ to actin filaments. The final concentrations of the components used in this experiments are as follows: IQGAP1$_{FL}$, 0.5 μM; polymerized actin, 1 μM; Ca^{2+} or EGTA, 220 μM; and calmodulin, 0.5 μM. Regardless of whether Ca^{2+} was present, in the absence of calmodulin ~70–80% of IQGAP1$_{FL}$ cosedimented with F-actin. In the presence of calmodulin plus Ca^{2+}, however, only ~50% of the IQGAP1$_{FL}$ pelleted, even when the IQGAP1$_{FL}$ was preincubated for 30 min with the actin filaments before adding the Ca^{2+}/calmodulin. Based on these results and the data presented earlier, we conclude that Ca^{2+}/calmodulin can form complexes with IQGAP1; such complexes have reduced affinity for actin filaments compared with Ca^{2+}/calmodulin-free IQGAP1, and prior association of IQGAP1 with F-actin does not provide protection against Ca^{2+}/calmodulin. It remains to be determined, however, if the initial binding of Ca^{2+}/calmodulin to IQGAP1 can occur while the latter is bound to F-actin or, alternatively, must await dissociation of IQGAP1 from F-actin.

Localization of IQGAP1-YFP in the Cell Cortex Is Reversibly Disrupted by Ca^{2+}—Prior immunofluorescence studies (4, 7) from several laboratories had indicated that IQGAP1 is typically most concentrated in the cell periphery, where it colocalizes with cortical actin filaments (2, 5). A key prediction of the *in vitro* biochemical data described here is that a rise in intracellular Ca^{2+} should remove IQGAP1 from the cortex. To test that prediction, NIH-3T3 cells were transiently transfected for expression of an IQGAP1-YFP fusion protein and exposed to the Ca^{2+} ionophore, A23187 and $CaCl_2$, alone or in combination. When used individually, neither the ionophore nor the $CaCl_2$ had any noticeable effect on the distribution of IQGAP1-YFP (not shown). When cells were exposed simultaneously to both agents, however, IQGAP1-YFP was rapidly removed from the cell cortex, an effect that was quickly reversed upon removal of the A23187 and $CaCl_2$.

These effects are illustrated in Fig. 8, which shows several frames from a time lapse movie of a single field of view photographed following addition of A23187 plus $CaCl_2$, and their subsequent removal. The movie was recorded using confocal imaging, and the plane of focus was near the lower surface of the cells. Cortical fluorescence decreased markedly within 5 min of exposure of the cells to A23187 and $CaCl_2$, especially at cell-cell contact sites, and recovered almost completely within 10 min after the A232187 and $CaCl_2$ were removed. QuickTime movies of both the forward and reverse reactions of the cells are available in the Supplemental Material. It is noteworthy that cortical F-actin remained intact during comparable exposures of cells to A23187 plus $CaCl_2$, as determined by staining of cells with AlexaFluor 488-phalloidin (Fig. 9). Thus, the displacement of IQGAP1-YFP from the cell cortex in response to elevated Ca^{2+} did not reflect a loss of cortical actin filaments.

One unexpected observation of these experiments was of intranuclear IQGAP1-YFP in occasional cells, an example of which is shown in Fig. 8 and the QuickTime movies (see the Supplemental Material). We do not yet understand the significance of this observation, but perhaps it reflects an association of IQGAP1 with intranuclear β-catenin. Regardless of what the explanation may prove to be, two other groups have published immunofluorescence micrographs of endogenous IQGAP1 that apparently was in the nucleus (2, 18).
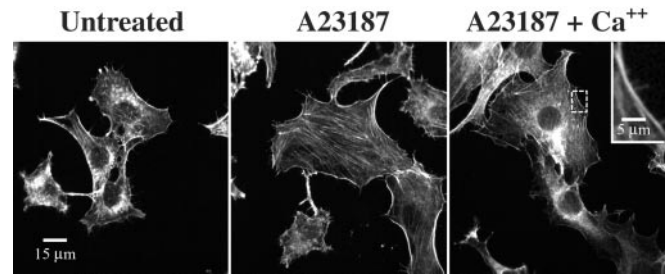
DISCUSSION

The initial report (5) that IQGAP1 binds to actin filaments included preliminary evidence for regulation of this activity by calmodulin, but the regulatory mechanism remained undefined. The study described here explains the broad details of that mechanism and suggests that the ability of IQGAP1 to bind actin filaments can be fine-tuned by calmodulin, acting through Ca^{2+}. We found that as the level of calmodulin associated with IQGAP1 increased, the F-actin binding activity of IQGAP1 progressively decreased and that Ca^{2+} potently enhanced the affinity of calmodulin for IQGAP1. Considering that IQGAP1 is most abundant intracellularly on cortical actin filaments (2, 4, 5, 7), these *in vitro* biochemical findings suggest that elevation of intracellular Ca^{2+} should promote reversible binding of calmodulin to IQGAP1 and, by extension, reversible withdrawal of IQGAP1 from the cortex. That is exactly what we observed for IQGAP1-YFP by time lapse fluorescence microscopy of live transfected cells whose intracellular Ca^{2+} levels were raised or decreased by the respective addition or removal of Ca^{2+} plus A23187. Fig. 10, which is based on the collective data presented here, summarizes how Ca^{2+}/calmodulin might negatively regulate interactions between IQGAP1 and cortical actin filaments in a reversible manner.

The question of how the other known cofactors for IQGAP1 impact on the regulation of its actin filament binding activity

+ Calcium / Recovery
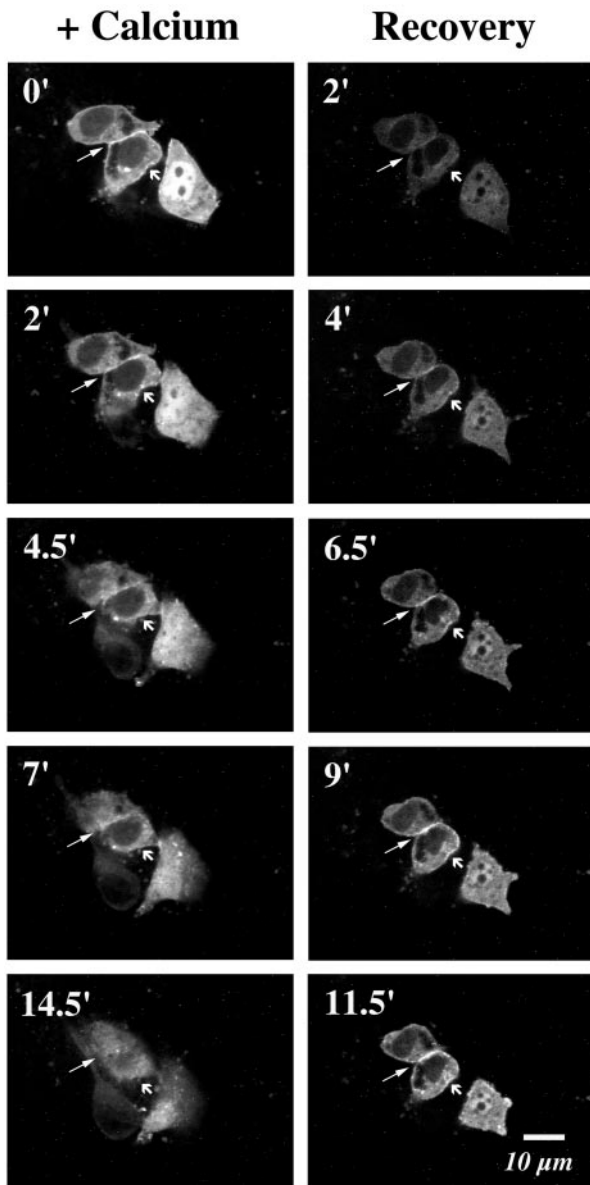
FIG. 8. **Ca²⁺ influx causes IQGAP1-YFP to dissociate reversibly from the cell cortex.** NIH-3T3 cells that expressed IQGAP1-YFP by transient transfection were exposed to the Ca²⁺ ionophore, A23187 (5 μM), plus 1 mM CaCl₂ in HBSS (+*Calcium*), and confocal fluorescence micrographs were taken at 30-s intervals for 22 min. The ionophore and Ca²⁺ were then replaced with Dulbecco's modified Eagle's medium plus 10% Cosmic calf serum, and 20 more images were captured at 30-s intervals (*Recovery*). For each panel, the time (in minutes) following addition of Ca²⁺ plus A23187 or initiation of the recovery step is shown in the *upper left corner*. Note that IQGAP1 localization at the cell periphery (*short arrows*) and sites of cell-cell contact (*long arrows*) was lost following Ca²⁺ influx and returned during the recovery step. Quick-Time videos of the complete Ca²⁺ addition and recovery time lapse sequences are available in the Supplemental Material.

FIG. 9. **Ca²⁺ influx does not cause cortical F-actin to disassemble.** NIH-3T3 cells were transferred from complete medium to Ca²⁺-free HBSS and then were incubated for 20 min without further supplements (*Untreated*), with 5 μM A23187, or with 5 μM A23187 plus 1 mM CaCl₂. Next, the cells were fixed and stained for F-actin using AlexaFluor 488-phalloidin. Note that cortical F-actin remained intact under all conditions.
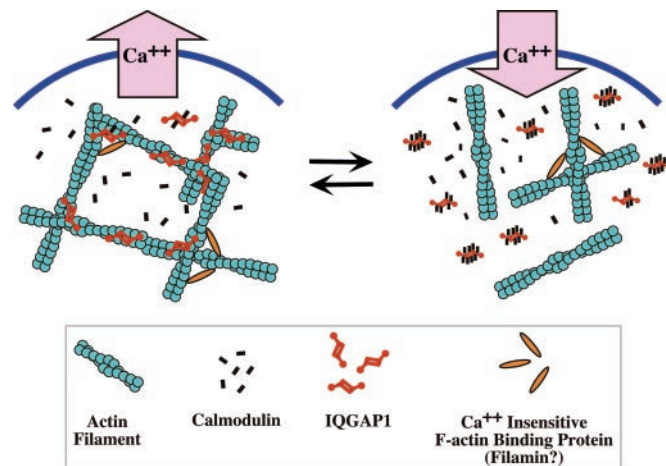
FIG. 10. **A model for the regulation of IQGAP1 binding to actin filaments in the cell cortex by Ca²⁺/calmodulin.** This model integrates the collective data shown in Figs. 1–9. Under conditions of low intracellular Ca²⁺, the amount of calmodulin bound to IQGAP1 is low, and the actin filament binding and gelation activities of IQGAP1 are maximal. When appropriate extracellular stimuli induce a reversible rise in intracellular Ca²⁺ levels, however, calmodulin binds much more avidly to IQGAP1 and inhibits its ability to bind actin filaments. Some actin filament gels may still persist under these conditions, however, because of the presence of Ca²⁺-insensitive cortical gelation factors, such as filamin (31).

must await further experimentation. In the meantime, an emerging theme from studies of IQGAP1 is how its binding partners compete with each other for association with their common ligand. For example, there are reports that Ca²⁺/calmodulin disrupts the association between IQGAP1 and E-cadherin (19) or activated Cdc42 (8) and that activated forms of Cdc42 or Rac1 inhibit binding of IQGAP1 to β-catenin (21). These findings, along with the results presented here, imply that multiple functions of IQGAP1 are regulated by its competitive interactions with a variety of signaling and structural proteins. Such functions may include the formation of filopodia

and lamellipodia, which involve assembly and reorganization of actin filaments, and are regulated, respectively, by Cdc42 and Rac1 (25, 26); cell-cell adhesion, which involves E-cadherin and β-catenin (27, 28); and β-catenin-mediated gene activation (27).

The deletion mutant, IQGAP1-(2–522), provides insight into the protein substructure that enables its native full-length counterpart to bind actin filaments and dimerize. The only known structural motifs in IQGAP1-(2–522) are the calponin homology domain, or CHD, and ~3.5 of the 6 putative coiled-coil repeats present in the full-length protein. Because IQGAP1-(2–522) was able to cross-link actin filaments into gels and bundles (Fig. 3), it must contain at least the minimum structural information for actin filament binding and dimerization. The ability of IQGAP1-(2–522) to bind actin filaments is consistent with an earlier report (21) that an even smaller N-terminal fragment of IQGAP1 is also capable of binding F-actin. This fragment, called IQGAP1$_{CHD}$, composed the first 232 amino acids of the full-length protein, extended shortly beyond the CHD, and was expressed as a fusion protein coupled to the C-terminal of GST (21).

Similarly, the lack of detectable effects of Ca²⁺/calmodulin on the F-actin binding properties of IQGAP1-(2–522) or

IQGAP1$_{\Delta IQ}$ (Figs. 3 and 5) implies that the sensitivity of IQGAP1$_{FL}$ to Ca^{2+}/calmodulin for actin filament binding depends on its IQ motifs. Interestingly, a prior study (9) of IQGAP1 included evidence that IQGAP1$_{CHD}$ can bind calmodulin in a Ca^{2+}-dependent, F-actin-sensitive manner. Although that result may seem at odds with the results presented here, it is noteworthy that the prior study clearly indicated that the affinity of Ca^{2+}/calmodulin for the IQ motifs was much greater than for IQGAP1$_{CHD}$ (9). The apparent discrepancy between our results and those reported earlier may reflect differences in the deletion mutants and actin binding assays used in the two studies. Regardless of what the explanation eventually proves to be, the collective evidence from both studies indicates that the ability of Ca^{2+}/calmodulin to suppress the F-actin binding activity of IQGAP1 is caused primarily by association of Ca^{2+}/calmodulin with the IQ motifs.

Calmodulin binding IQ motifs contain the consensus sequence IQ*XXX*RG*XXX*(R) (29) and have been proposed to fall into two classes. Incomplete IQ motifs are defined as lacking the C-terminal arginine and reportedly have a much higher affinity for Ca^{2+}/calmodulin than for calmodulin alone. In contrast, complete IQ motifs are defined as containing the distal arginine and are thought to bind well to free calmodulin (30). By these definitions, each IQGAP1 dimer contains 6 complete and 2 incomplete IQ domains. In the presence of EGTA, a 1:1 molar ratio of calmodulin to IQGAP1$_{FL}$ dimer had no detectable effect on the actin gelation or binding activity of IQGAP1$_{FL}$ (Fig. 3), and a 10-fold excess of calmodulin caused only an ~20% reduction in the amount of IQGAP1$_{FL}$ that could bind F-actin (Fig. 4). In the presence of Ca^{2+}, however, a 1:1 ratio of calmodulin to IQGAP1$_{FL}$ dimer prevented gelation of actin filaments (Fig. 3). Likewise, addition of Ca^{2+} to mixtures containing either 1:1 or 10:1 ratios of calmodulin to IQGAP1$_{FL}$ reduced the amount of IQGAP1$_{FL}$ found in actin pellets by ~45 and ~80%, respectively.

The collective data presented here suggest two possible routes, which may not be mutually exclusive, by which calmodulin can suppress the F-actin binding activity of IQGAP1. One possibility is that the affinity of IQGAP1 for F-actin is inversely proportional to the number of its bound calmodulin, at least to a first approximation. Arguing in favor of this hypothesis is the finding that in the presence of Ca^{2+}, the level of F-actin binding by IQGAP1$_{FL}$ was inhibited ~40% by equimolar calmodulin but by ~70% when a 10-fold molar excess of calmodulin was present (Fig. 4). Interestingly, all 8 IQ motifs in IQGAP1 were occupied by calmodulin in the latter case (Fig. 6), indicating that IQGAP1 can retain a low F-actin binding activity even when it is saturated with calmodulin. An alternative model was suggested by the finding that ~25% of purified native IQGAP1 was associated with equimolar calmodulin and did not bind F-actin *in vitro* (Fig. 1). This result raises the possibility that binding of a single calmodulin molecule to an IQGAP1 dimer can prevent the IQGAP1 from binding to an actin filament. Moreover, it invites speculation that calmodulin must be associated with a particular IQ motif, perhaps an incomplete IQ motif, in order to exert such a drastic effect. Even though the native IQGAP1 was purified from bovine adrenal tissue in the presence of EGTA, it is possible that Ca^{2+}/calmodulin-IQGAP1 complexes that existed *in vivo* were able to remain intact throughout the purification procedure and, as a result, retain low F-actin binding activity *in vitro*. Although both of these models are worthy of consideration in light of the existing data, it is clear that further studies of the IQ motifs of IQGAP1 will be required to determine in greater detail how calmodulin regulates its binding to F-actin.

In the absence of calmodulin, Ca^{2+} caused a slight inhibition of F-actin gelation by IQGAP1$_{FL}$ but not IQGAP1-(2–522) (Fig. 3). Reportedly, Ca^{2+} can directly associate with IQGAP1$_{CHD}$ (9). It is therefore possible that direct binding of Ca^{2+} somewhere within the N-terminal region of IQGAP1$_{FL}$ slightly inhibited its affinity for actin filaments. Why such an effect was not observed for IQGAP1-(2–522) remains a mystery. One possible explanation is that the C-terminal of IQGAP1$_{FL}$, which is missing in IQGAP1-(2–522), can partially block the CHD when Ca^{2+} is bound to the N-terminal region of the protein. Another plausible explanation is that the methionine that marks the N-terminal amino acid residue in IQGAP1$_{FL}$ and is absent from IQGAP1-(2–522) is required for calmodulin-independent binding of Ca^{2+}. Although Ca^{2+} affected IQGAP1$_{FL}$ gelation activity, it had no detectable effect in a pelleting assay for F-actin binding (Fig. 4). Because falling ball viscometry is thought to be more sensitive than the pelleting assay, its possible that the slight Ca^{2+} effect observed in the gelation assay was too small to be detected in the pelleting assay.

There is one discrepancy between the results we present here and those we described earlier (5) for the effects of Ca^{2+} and calmodulin on IQGAP1. The F-actin binding activity of IQGAP1 was originally reported to be comparably inhibited by calmodulin or Ca^{2+}/calmodulin (5), but we now present evidence that Ca^{2+}/calmodulin is a much more potent inhibitor than calmodulin alone (see Figs. 3*B* and 4). This disparity probably reflects two major differences in experimental design between our earlier work (5) and the work described here. First, we used native bovine adrenal IQGAP1 originally (5) and recombinant human IQGAP1$_{FL}$ more recently. The recombinant protein consistently appeared to be much purer than its native counterpart by SDS-PAGE (compare Fig. 2 in this paper with Fig. 3*A* in Ref. 5) and was also demonstrated to contain substantially less calmodulin. Because IQGAP1$_{FL}$ was produced by baculovirus-directed overexpression in insect cells, it is likely that the purified recombinant protein also contained lower levels than the native protein of other cofactors that may influence how Ca^{2+} and calmodulin affect F-actin binding by IQGAP1. Such cofactors are known to include the small G proteins Cdc42 and Rac1 (2–4), β-catenin (18), and E-cadherin (18, 19), and others may remain to be discovered. These considerations lead us to believe that protein-protein interactions involving IQGAP1 can be dissected more systematically and accurately using recombinant, as opposed to native, versions of the protein.

The other substantive difference between our original and present experiments is that calmodulin was previously used at a 5:1 molar ratio to the IQ motifs on IQGAP1 but at only a 1:8 or 5:4 molar ratio for the current study. The new data shown in Fig. 4 illuminates the importance of this difference. In particular, the binding of IQGAP1 to F-actin was not inhibited at a 1:8 ratio of calmodulin to IQ motifs when Ca^{2+} was absent (Fig. 4, *lane/pellet fraction 2*) but was inhibited by ~40% at the same calmodulin concentration in the presence of Ca^{2+} (*lane/pellet fraction 5*) or at a 10-fold higher calmodulin concentration in the absence of Ca^{2+} (*lane/pellet fraction 3*). Furthermore, the inhibition was even more pronounced at the higher calmodulin concentration when Ca^{2+} was also present (*lane/pellet fraction 6*). These data support the view that calmodulin inhibits the binding of IQGAP1 to F-actin and that Ca^{2+} increases the affinity of calmodulin for IQGAP1. Thus, the effects of calmodulin on the F-actin binding properties of IQGAP1 may be insensitive to Ca^{2+} when calmodulin is present in vast excess to IQGAP1, as was the case in our earlier study (5) but not our present study.

Now that regulation of the F-actin binding activity of IQGAP1 by Ca^{2+} and calmodulin is understood in considerable

detail, new questions about the biochemical and cell biological properties of IQGAP1 will rise to the forefront. In the most general sense, it will be important to develop an understanding of how the various binding partners of IQGAP1, individually and collectively, affect its numerous functions. Because the proteins that consort with IQGAP1 have been implicated in activities as diverse as cellular motility and morphogenesis, cell-cell adhesion, and gene regulation, it may be useful to think of IQGAP1 as a signal integration protein that can mount an array of specific responses to diverse extracellular and intracellular signals. The particular combination of signals that is operative at any moment may determine which cofactors bind to IQGAP1 at that time and, by extension, may specify the predominant functions of IQGAP1 while those signals remain strong.

REFERENCES

1. Weissbach, L., Settleman, J., Kalady, M. F., Snijders, A. J., Murthy, A. E., Yan, Y.-X., and Bernards, A. (1994) *J. Biol. Chem.* **269,** 20517–20521
2. Hart, M. J., Callow, M. G., Souza, B., and Polakis, P. (1996) *EMBO J.* **15,** 2997–3005
3. McCallum, S. J., Wu, W. J., and Cerione, R. A. (1996) *J. Biol. Chem.* **271,** 21732–21737
4. Kuroda, S., Fukata, M., Kobayashi, K., Nakafuku, M., Nomura, N., Iwamatsu, A., and Kaibuchi, K. (1996) *J. Biol. Chem.* **271,** 23363–23367
5. Bashour, A.-M., Fullerton, A. T., Hart, M. J., and Bloom, G. S. (1997) *J. Cell Biol.* **137,** 1555–1566
6. Fukata, M., Kuroda, S., Fujii, K., Nakamura, T., Shoji, I., Matsuura, Y., Okawa, K., Iwamatsu, A., Kikuchi, A., and Kaibuchi, K. (1997) *J. Biol. Chem.* **272,** 29579–29583
7. Erickson, J. W., Cerione, R. A., and Hart, M. J. (1997) *J. Biol. Chem.* **272,** 24443–24447
8. Joyal, J. L., Annan, R. S., Ho, Y.-D., Huddleston, M. E., Carr, S. A., Hart, M. J., and Sacks, D. B. (1997) *J. Biol. Chem.* **272,** 15419–15425
9. Ho, Y. D., Joyal, J. L., Li, Z., and Sacks, D. B. (1999) *J. Biol. Chem.* **274,** 464–470
10. Brill, S., Li, S., Lyman, C. W., Church, D. M., Wasmuth, J. J., Weissbach, L., Bernards, A., and Snijders, A. (1996) *Mol. Cell. Biol.* **16,** 4869–4878
11. Venturelli, C. R., Kuznetsov, S., Salgado, L. M., and Bosch, T. C. (2000) *Dev. Genes Evol.* **210,** 458–463
12. Faix, J., and Dittrich, W. (1996) *FEBS Lett.* **394,** 251–257
13. Adachi, H., Takahashi, Y., Hasebe, T., Shirouzu, M., Yokoyama, S., and Sutoh, K. (1997) *J. Cell Biol.* **137,** 891–898
14. Lee, S., Escalante, R., and Firtel, R. A. (1997) *Development* **124,** 983–996
15. Epp, J. A., and Chant, J. (1997) *Curr. Biol.* **7,** 921–929
16. Lippincott, J., and Li, R. (1998) *J. Cell Biol.* **140,** 355–366
17. Osman, M. A., and Cerione, R. A. (1998) *J. Cell Biol.* **142,** 443–455
18. Kuroda, S., Fukata, M., Nakagawa, M., Fujii, K., Nakamura, T., Ookubo, T., Izawa, I., Nagase, T., Nomura, N., Tani, H., Shoji, I., Matsuura, Y., Yonehara, S., and Kaibuchi, K. (1998) *Science* **281,** 832–835
19. Li, Z., Kim, S. H., Higgins, J. M., Brenner, M. B., and Sacks, D. B. (1999) *J. Biol. Chem.* **274,** 37885–37892
20. Weissbach, L., Bernards, A., and Herion, D. W. (1998) *Biochem. Biophys. Res. Commun.* **251,** 269–276
21. Fukata, M., Kuroda, S., Nakagawa, M., Kawajiri, A., Itoh, N., Shoji, I., Matsuura, Y., Yonehara, S., Fujisawa, H., Kikuchi, A., and Kaibuchi, K. (1999) *J. Biol. Chem.* **274,** 26044–26050
22. Laemmli, U. K. (1970) *Nature* **227,** 680–685
23. Pfister, K. K., Wagner, M. C., Stenoien, D. A., Brady, S. T., and Bloom, G. S. (1989) *J. Cell Biol.* **108,** 1453–1463
24. Bloom, G. S., Richards, B. W., Leopold, P. L., Ritchey, D. M., and Brady, S. T. (1993) *J. Cell Biol.* **120,** 467–476
25. Nobes, C. D., and Hall, A. (1995) *Cell* **81,** 53–62
26. Ridley, A. J., Paterson, H. F., Johnston, C. L., Diekman, D., and Hall, A. (1992) *Cell* **70,** 401–410
27. Ben-Ze'ev, A., Shtutman, M., and Zhurinsky, J. (2000) *Exp. Cell Res.* **261,** 75–82
28. Gumbiner, B. M. (1996) *Cell* **84,** 345–357
29. Cheney, R. E., and Mooseker, M. S. (1992) *Curr. Opin. Cell Biol.* **4,** 27–35
30. Houdusse, A., and Cohen, C. (1995) *Proc. Natl. Acad. Sci. U. S. A.* **92,** 10644–10647
31. Weihing, R. R. (1985) *Can. J. Biochem. Cell Biol.* **63,** 397–413